Calcif Tissue Int (2016) 98:566–572
DOI 10.1007/s00223-016-0110-1

ORIGINAL RESEARCH

Osteogenesis Imperfecta Type VI in Individuals from Northern Canada

Leanne Ward[1] · Ghalib Bardai[2] · Pierre Moffatt[2] · Hadil Al-Jallad[2] · Pamela Trejo[2] · Francis H Glorieux[2] · Frank Rauch[2]

Received: 26 October 2015 / Accepted: 13 January 2016 / Published online: 27 January 2016

Abstract Osteogenesis imperfecta (OI) type VI is a recessively inherited form of OI that is caused by mutations in *SERPINF1*, the gene coding for pigment-epithelium derived factor (PEDF). Here, we report on two apparently unrelated children with OI type VI who had the same unusual homozygous variant in intron 6 of *SERPINF1* (c.787-10C>G). This variant created a novel splice site that led to the in-frame addition of three amino acids to PEDF (p.Lys262_Ile263insLeuSerGln). Western blotting showed that skin fibroblasts with this mutation produced PEDF but failed to secrete it. Both children were treated with intravenous bisphosphonates, but the treatment of Individual 1 was switched to subcutaneous injections of denosumab (dose 1 mg per kg body weight, repeated every 3 months). An iliac bone sample obtained after 5 denosumab injections (and 3 months after the last injection) showed no change in the increased osteoid parameters that are typical of OI type VI, but the number of osteoclasts in trabecular bone was markedly increased. This suggests that the effect of denosumab on osteoclast suppression is of shorter duration in children with OI type VI than what has previously been reported on adults with osteoporosis.

Keywords Children · Fractures · Osteogenesis imperfecta · Pigment-epithelium derived factor · *SERPINF1*

✉ Frank Rauch
frauch@shriners.mcgill.ca

[1] Childrens Hospital of Eastern Ontario, Ottawa, ON, Canada

[2] Shriners Hospital for Children and McGill University, 1529 Cedar Avenue, Montreal, QC H3G 1A6, Canada

Introduction

Osteogenesis imperfecta (OI) type VI (MIM 613982) is a rare form of OI that we first described as a separate disease entity in 2002 [1]. Whereas the most common OI types are transmitted as autosomal dominant traits due to mutations in *COL1A1* or *COL1A2*, OI type VI is an autosomal recessive disorder. It was initially distinguished from other OI types based on bone histological characteristics that are not usually present in OI, namely the presence of a large amount of unmineralized bone matrix and the appearance of 'fish scale' lamellation when the bone is examined by polarized light microscopy [1]. Children with OI type VI usually appear to be healthy at birth and sustain fractures only after the age of 6 months. Symptomatic antiresorptive treatment approaches with either intravenous bisphosphonates or subcutaneous injections of denosumab have been proposed, in an attempt to increase bone mass and to decrease fracture rates [2, 3].

We previously reported that OI type VI is caused by loss-of-function mutation in *SERPINF1* [MIM 172860, NM_002615.5], the gene coding for pigment-epithelium derived factor [PEDF, NP_002606.3] [4], and that patients with OI type VI had levels of circulating PEDF at or below the detection limit [5]. This was true both for individuals with homozygous stop or frameshift mutations and for patients with in-frame mutations in *SERPINF1* [6]. In total, 18 different *SERPINF1* mutations affecting about 30 individuals with OI type VI have been reported and are listed in the Osteogenesis Imperfecta Variant Database (http://www.le.ac.uk/ge/collagen/). Heterozygous carriers are asymptomatic and have normal bone density despite slightly low serum PEDF [7].

Here, we report on two apparently unrelated children with OI type VI from the same region in northern Canada in whom an unusual intronic variant led to the creation of a cryptic splice site in *SERPINF1* and an in-frame addition of three

amino acids to PEDF. One of the two children was treated with denosumab and this report contains the first bone histomorphometric observations in a child with OI type VI receiving this therapy.

Subjects and Methods

The individuals described here were followed at Shriners Hospital for Children in Montreal and at the Childrens Hospital of Eastern Ontario in Ottawa. Clinical information was obtained through retrospective chart review. Genetic investigations were performed at Shriners Hospital for Children in Montreal, Canada, after informed consent, with approval from the Institutional Review Board of McGill University.

Dual-energy X-ray absorptiometry was performed in the anterior–posterior direction at the lumbar spine (L1–L4) using a Hologic QDR Discovery device (Hologic Inc., Waltham, MA, USA). Lumbar spine areal bone mineral density (BMD) results were transformed to age- and gender-specific z-scores using published reference data [8, 9].

Iliac bone samples were obtained in Individual 1 at a site 2 cm posterior of the superior anterior iliac spine, following tetracycline double labeling, as described [10]. Sample preparation and histomorphometric analyses were performed using previously described procedures [10]. Results were compared to the average value of the age-specific reference range using data established in our laboratory [10].

Human primary skin fibroblasts from a control and the proband were grown in αMEM supplemented with 10 % fetal bovine serum, GlutaMAX (final concentration: 2 mM), 100 units/mL penicillin, 100 μg/ml streptomycin and 2 μg/ml amphotericin B. These cells were plated at 100,000 cells per well in 6-well tissue culture plates. Total RNA was extracted from confluent fibroblasts using the Trizol reagent (Invitrogen) and cDNA was obtained.

Genomic DNA sequencing was performed by semiconductor-based next-generation sequencing using an Ion Torrent PGM device (Life Technologies), as described [11], and with a 3100 DNA sequencer (Applied Biosystems, Foster City, USA). Sequencing of cDNA was performed at the McGill and Genome Quebec Innovation Center using a 3130xl genetic analyzer (Applied Biosystems, Foster City, USA).

Results

Clinical Descriptions

Individual 1

The boy was born prematurely after 34 weeks of uncomplicated gestation. He was the first child of healthy parents. Birth weight was 2540 g (75th percentile for gestational age). No abnormalities were noted at birth, and postnatal development was initially normal. He was able to pull up to stand at 10 months of age. The first fracture (right tibia) occurred at the age of 11 months. He was first examined at a specialized center at 14 months of age, after he had sustained 5 long-bone fractures (both femurs, both humeri, left radius) and one compression fracture of thoracic vertebra 12. At that age, height and weight were at the 50th percentile. Bowing of femurs and humeri was noted but he had normal-appearing teeth and white sclera. There was mild joint hyperlaxity. Dual-energy X-ray absorptiometry of lumbar vertebrae revealed an age-specific areal BMD z-score of −1.7. A skull x-ray showed no evidence of Wormian bones. Biochemical parameters of bone and mineral metabolism were normal. The serum concentration of 25-hydroxyvitamin D was 124 nmol/L.

An iliac bone biopsy sample was obtained and showed typical features of OI type VI, with ‘fish scale lamellation’ and an increased amount of unmineralized osteoid in the trabecular bone compartment, with osteoid making up 22.5 % of trabecular bone (Norm: 1.6–6.4 %) and failure to take up tetracycline label (Table 1).

Treatment with intravenous zoledronic acid at a dose of 0.0125 mg per kg body weight was started at 17 months of age and a second infusion (dose: 0.025 mg per kg body weight) was given 4 months later. However, fracture rate continued to be high (two femur fractures and one forearm fracture in the 6 months following the first zoledronic acid infusion) and zoledronic acid was therefore discontinued after the second infusion. Treatment with subcutaneous injection of denosumab (1 mg per kg body weight, a similar weight-adjusted dose as the standard 60 mg dose given in adults) was initiated at 23 months of age and continued at the same dose every 3 months, for a total of 4 doses during the observation interval reported here. Denosumab was tolerated well, with no episodes of hypocalcemia or hypercalcemia in the setting of adequate dietary intake of calcium and supplemental vitamin D, plus calcium supplementation in the 5 days following each denosumab injection. Nevertheless, fractures continued to occur frequently. Radiographs at the age of 25 months revealed multiple vertebral compression fractures as well as lower extremity fractures (Fig. 1a–c). At the last follow up visit at the age of 3 years and 3 months, the lumbar spine areal BMD z-score was −3.9 SD. A second iliac bone biopsy sample was obtained at that time, 3 months after the last dose of denosumab. Histomorphometric analysis showed absence of tetracycline label uptake and therefore inability to measure dynamic bone formation parameters. The amount of osteoid remained elevated (Fig. 1d; Table 1). Surprisingly, this second bone sample contained far more osteoclasts than the pre-treatment sample (Table 1).

Table 1 Results of iliac bone histomorphometry in Individual 1 before and after treatment with denosumab

	Pre-treatment	Post-treatment	Reference data
Osteoid thickness (μm)	12.6	13.4	5.8 (1.4)
Osteoid surface per bone surface (%)	63	64	34 (7)
Number of osteoclasts per bone perimeter (/mm)	0.1	1.8	0.4 (0.2)
Osteoclast surface per bone surface (%)	0.04	4.2	1.1 (0.8)

The post-treatment sample was obtained 3 months after the last denosumab injection

Reference data were taken from Glorieux et al. [10]

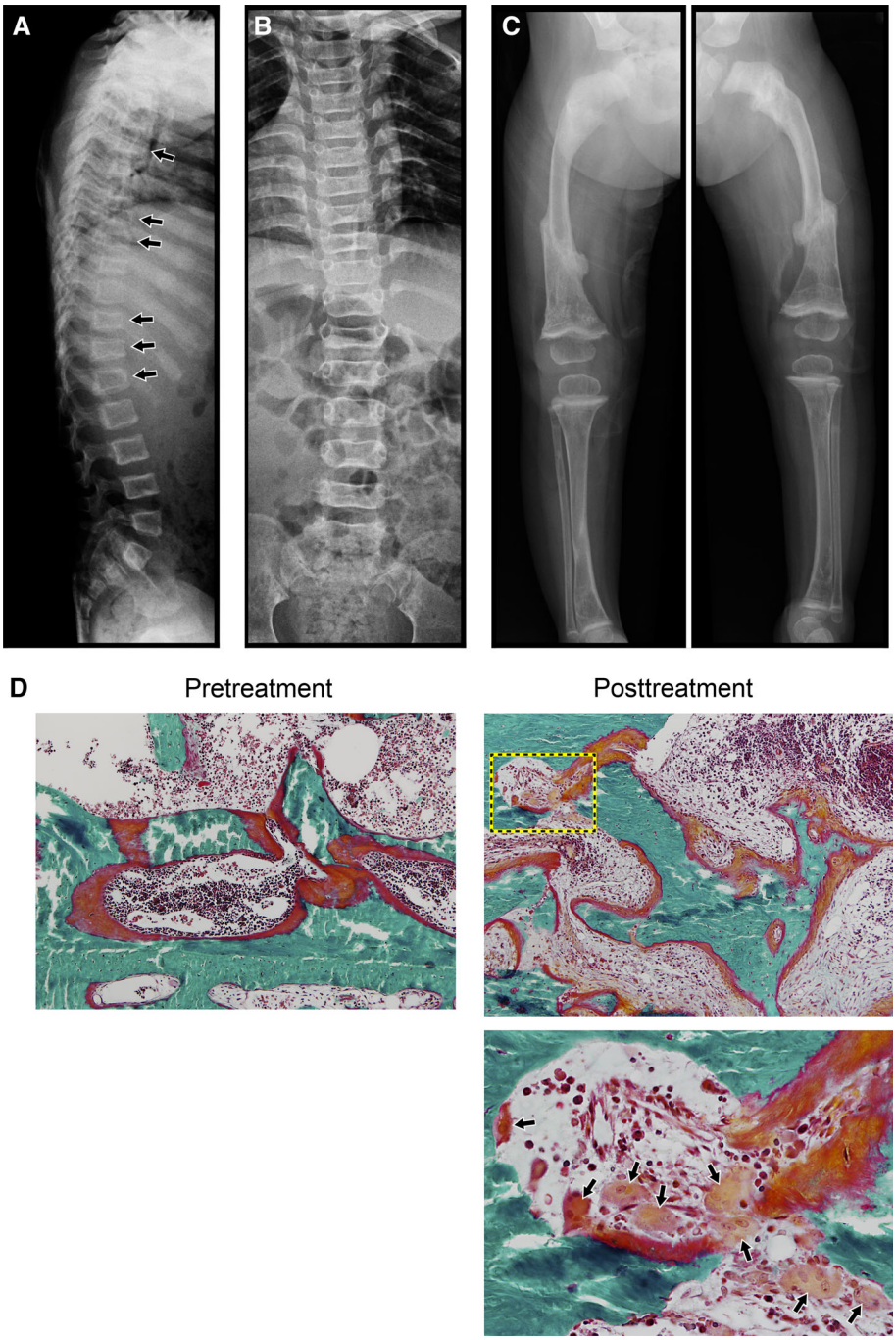

Fig. 1 **a–c** Radiographs at 2.1 years of age. **a** Lateral view of the spine, showing multiple vertebral compression fractures indicated by *arrows*. **b** Anteroposterior view of the spine. The majority of vertebral bodies have a flattened appearance. **c** Lower extremities with incompletely healed bilateral femur fractures. The sclerotic metaphyseal areas are due to prior treatment with zoledronate. **d** Iliac bone sample of Individual 1 prior to antiresorptive therapy (*left panel*; age 1.4 years) and after therapy (*right panels*; age 3.2 years). The amount of osteoid appears similar after therapy, but more osteoclasts are seen on mineralized bone surfaces (*lower right panel*, *arrows*)

Individual 2

This girl had been included in a previous report, where we had noted that she had undetectable PEDF serum levels but at the time we had failed to detect a pathogenic *SERPINF1* variant in her genomic DNA [5]. She was born at term, after an uncomplicated pregnancy. Both parents were from the same area in northern Canada and were healthy. No limb deformities or other abnormalities were noted at birth. Individual 2 sustained her first fracture (right tibia) when she was 12 months old. Physical examination revealed normal-appearing teeth and mild joint hyperlaxity. After four more long-bone fractures had occurred, treatment with intravenous pamidronate was started at 5 years of age. At that time, the age- and sex-dependent z-score for areal BMD at the lumbar spine was −3.9 on dual-energy X-ray absorptiometry. Pamidronate treatment was maintained for 8 years. Nevertheless, she developed severe scoliosis and eventually underwent spinal fusion surgery at the age of 19 years. Final height was 139 cm. As a young adult, she requires a wheelchair for all mobility.

Laboratory Results

Semiconductor-based sequencing of genomic DNA using a metabolic bone panel [11] revealed that Individual 1 had a homozygous c.787-10C>G variant in intron 6 of *SERPINF1* (Fig. 2a). No other potentially disease-causing variants were found in the genes that were known to be associated with OI at the time of these analyses (*COL1A1, COL1A2, CRTAP, LEPRE1, PPIB, SERPINH1, FKBP10, PLOD2, SP7, SERPINF1, BMP1, TMEM38B, IFITM5, LRP5*). Sanger sequencing confirmed that Individual 1 was homozygous for the c.787-10C>G variant, whereas his mother was a heterozygous carrier. The father was not available for evaluation. Sanger sequencing of intron 6/exon 7 in genomic DNA of Individual 2 showed the presence of the same homozygous mutation as was found in Individual 1 (Fig. 2b).

The *SERPINF1* c.787-10C>G variant was not listed in either the Osteogenesis Imperfecta Variant Database (accessed 21-Oct-2015) nor in the ExAC Browser database (version 0.3). The Human Splice Finder algorithm (version 3.0) predicted that the variant introduced a new splice acceptor site and abolished the wild-type splice acceptor site of *SERPINF1* exon 7. To evaluate the effect of the variant on splicing, we obtained skin fibroblasts from Individual 1 and extracted mRNA. Real-time PCR showed that the amount of *SERPINF1* cDNA (relative to GAPDH) in Individual 1 was three orders of magnitude lower than in controls (data not shown). Nevertheless, PCR amplification of cDNA using a forward primer in *SERPINF1* exon 4 and a reverse primer in exon 7 resulted in a PCR product of the expected length. Sequencing of this PCR product showed that 9 nucleotides of intron 6 sequence had been included into exon 7 (Fig. 2c), resulting in the in-frame addition of 3 amino acids (p.Lys262_Ile263insLeuSerGln). Immunoblotting showed that skin fibroblasts of Individual 1 contained PEDF in the cell layer, but PEDF was not detected in the conditioned medium under the conditions used (Fig. 2d).

Discussion

In this assessment of two apparently unrelated children with OI type VI, we found the same unusual intronic variant in *SERPINF1*. This variant created a cryptic splice site that led to the in-frame inclusion of 9 intronic nucleotides to the *SERPINF1* transcript and thus added 3 amino acids to PEDF. As the variant did not affect the immediate splice site sequence, it had been missed in our earlier studies on Individual 2 [5]. Similar to what we had observed in some other in-frame *SERPINF1* variants [6], mutated PEDF was detectable in the cell layer of cultured skin fibroblasts but not in the cultured medium, suggesting that the sequence change prevented PEDF secretion.

Even though there was no known family relationship between the two children, they both were born to parents from the same area in northern Canada. It therefore appears likely that there is a founder effect for the c.787-10C>G *SERPINF1* variant in this community and that the two children described here share a common ancestor who carried the variant.

The results of cDNA sequencing showed that the c.787-10C>G *SERPINF1* variant led to the use of a new splice site in intron 6 and the in-frame addition of 9 nucleotides. Real-time PCR indicated that *SERPINF1* transcript levels were markedly decreased in fibroblasts affected by the c.787-10C>G variant. As transcript decay is not usually expected in the presence of in-frame variants, this observation suggests that the variant does not only lead to the inclusion of 9 nucleotides into the *SERPINF1* transcripts but has alternative splice outcomes as well. One possibility is exon skipping, which is a common outcome of splice site variants [12]. Skipping of *SERPINF1* exon 7 (length: 211 nucleotides) would lead to a frameshift, nonsense-mediated decay of *SERPINF1* mRNA and thus low transcript levels.

The mechanism whereby *SERPINF1* variants lead to bone fragility and the mineralization defect that is characteristic of OI type VI is not clear at present. All individuals with OI type VI that have been investigated until now have PEDF serum levels at or below the limit of detection [5], suggesting that the absence of extracellular PEDF plays an important role in the pathogenic mechanism of the disorder. The uniformity of the effect of *SERPINF1*

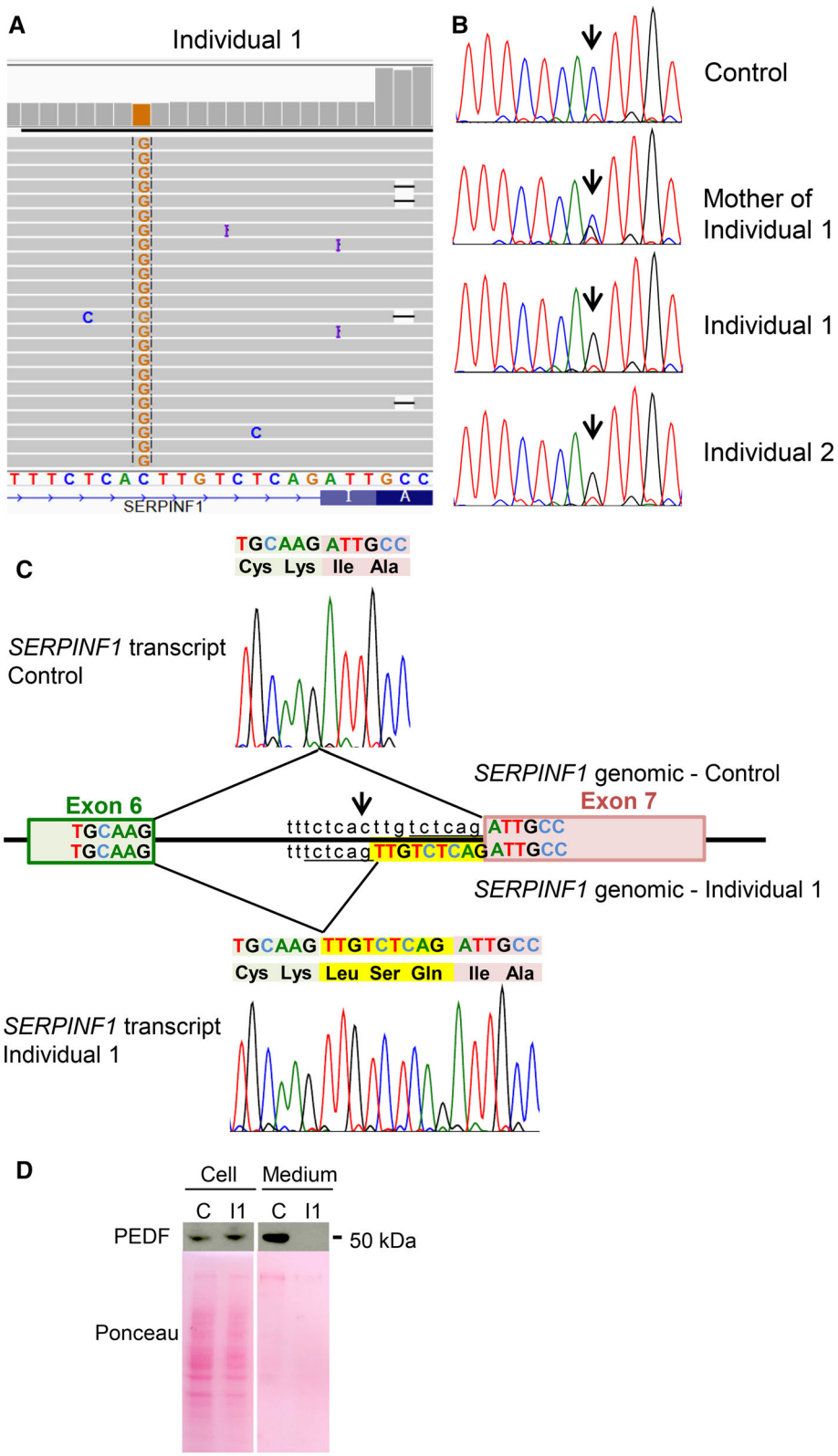

Fig. 2 **a** Integrative Genomics Viewer representation of semiconductor-based sequencing result in Individual 1, showing a homozygous c.787-10C>G variant in *SERPINF1*. **b** Sanger sequencing result of *SERPINF1* intron 6/exon 7 splice site mutation in *SERPINF1*. Individuals 1 and 2 are homozygous for c.787-10C>G, the mother of Individual 1 is heterozygous. **c** Sanger sequencing of skin fibroblast cDNA from a control (*upper part* of the panel) and from Individual 1 (*lower part*). The *middle part* indicates genomic DNA sequence in the *SERPINF1* intron 6/exon 7 region. The nucleotide affected by the c.787-10C>G mutation is indicated by an *arrow*. This mutation introduces a sequence of 6 nucleotides (*underlined*) from position −16 to −11 in intron 6 that is identical to nucleotides −6 to −1 in the wild-type sequence, thus creating a cryptic splice site. **d** Immunoblot of PEDF protein in the cell layer and in the conditioned medium of skin fibroblasts of Individual 1 (I1) and a control (**c**). In Individual 1, PEDF is detectable in the cell layer but not in the conditioned medium. Ponceau staining (*bottom*) shows similar loading between the control and Individual 1

mutations on PEDF secretion might also explain why no genotype-phenotype correlations have been noted until now. In vitro assays have shown that PEDF can interact with collagen type I [13]. It is therefore possible that the absence of PEDF affects the structure or function of extracellular collagen type I. In line with this view, OI type

VI is associated with marked hypermineralization on the material bone level [14], which is similar to what is seen in OI caused by mutations in the collagen type I encoding genes [15].

Concerning bone-strengthening medical treatment of OI type VI, we have previously noted that intravenous bisphosphonate therapy is less effective in OI type VI than in other types of OI [2]. Subsequently, encouraging observations were reported with a newer antiresorptive treatment approach using denosumab [3, 16]. However, given the small number of patients with OI type VI, the information on this approach is necessarily very limited and the efficacy of this approach is difficult to judge.

Individual 1 of the present report continued to have frequent fractures after treatment with intravenous zoledronic acid had been started and therefore a treatment attempt with denosumab was made. The bone sample obtained after 5 injections of denosumab (and 3 months after the last dose of denosumab) did not show any changes in the large amount of unmineralized osteoid that was present prior to medical therapy. This is in contrast to observations in women with postmenopausal osteoporosis, where treatment with denosumab was associated with a marked decrease in the amount of osteoid [17]. The lack of response in osteoid parameters in our patient may reflect the fact that in OI type VI the amount of osteoid is increased due to a mineralization defect, which is presumably not affected by denosumab, whereas in postmenopausal osteoporosis the amount of osteoid reflects the rate of bone turnover, which is markedly decreased by denosumab.

OI type VI is characterized on the bone tissue and material levels by marked abnormalities in 'bone quality', such as increased calcium content of the bone matrix, disorganized collagen fibrils and unusual size, shape and arrangement of mineral particles [14]. In contrast, in our initial description of OI type VI, we reported that osteoclast number of children with OI type VI is similar to that of age-matched controls [1]. As antiresorptive treatment inhibits osteoclast activity but is unlikely to correct these bone quality issues, antiresorptive treatment in OI type VI can be expected to bring about limited improvements at best. It is surprising, however, that Individual 1 had a large number of osteoclasts in the bone sample that was obtained after denosumab therapy. In postmenopausal women denosumab decreased osteoclast number, but serum markers of bone resorption rebounded markedly between 6 and 9 months following the last denosumab injection [17, 18]. As Individual 1 had elevated osteoclast numbers already at 3 months after the last denosumab injection, it seems possible that the suppressive effect of denosumab on osteoclasts is of shorter duration in children with OI type VI than in postmenopausal women with osteoporosis.

In conclusion, we found an unusual *SERPINF1* splice variant in two children with OI type VI that led to an in-frame addition of three amino acids to PEDF and a defect in PEDF secretion. Treatment with denosumab in one child did not affect the increased amount of osteoid in iliac bone and a large number osteoclasts was present 3 months after the last denosumab injection. This suggests that the effect of denosumab on osteoclast suppression is of shorter duration in children with OI type VI than what has previously been reported for adults with osteoporosis.

Acknowledgments This study was supported by the Shriners of North America and the Fonds de recherche du Québec—Santé. We thank Mark Lepik for the preparation of the figures and Patty Mason for technical assistance. F.R. received support from the Chercheur-Boursier Clinicien program of the Fonds de Recherche du Québec—Santé. This study was supported by the Shriners of North America.

Compliance with Ethical Standards

Conflict of Interests Frank Rauch received support from the Chercheur-Boursier Clinicien program of the Fonds de Recherche du Québec—Santé and has received consultancy fees from Genzyme Inc and Alexion Inc. Francis H Glorieux has received consultancy fees from Novartis Inc, Amgen Inc and Alexion Inc. Leanne Ward, Ghalib Bardai, Pierre Moffatt, Hadil Al-Jallad, and Pamela Trejo declare no conflict of interest.

Human and Animal Rights and Informed Consent All procedures followed were in accordance with the ethical standards of the responsible committee on human experimentation (institutional and national) and with the Helsinki Declaration of 1975, as revised in 2000. Informed consent was obtained from study participants or the legal guardians.

References

1. Glorieux FH, Ward LM, Rauch F, Lalic L, Roughley PJ, Travers R (2002) Osteogenesis imperfecta type VI: a form of brittle bone disease with a mineralization defect. J Bone Miner Res 17:30–38
2. Land C, Rauch F, Travers R, Glorieux FH (2007) Osteogenesis imperfecta type VI in childhood and adolescence: effects of cyclical intravenous pamidronate treatment. Bone 40:638–644
3. Semler O, Netzer C, Hoyer-Kuhn H, Becker J, Eysel P, Schoenau E (2012) First use of the RANKL antibody denosumab in osteogenesis imperfecta type VI. J Musculoskelet Neuronal Interact 12:183–188
4. Homan EP, Rauch F, Grafe I, Lietman C, Doll JA, Dawson B, Bertin T, Napierala D, Morello R, Gibbs R, White L, Miki R, Cohn DH, Crawford S, Travers R, Glorieux FH, Lee B (2011) Mutations in SERPINF1 cause osteogenesis imperfecta type VI. J Bone Miner Res 26:2798–2803
5. Rauch F, Husseini A, Roughley P, Glorieux FH, Moffatt P (2012) Lack of circulating pigment epithelium-derived factor is a marker of osteogenesis imperfecta type VI. J Clin Endocrinol Metab 97:E1550–E1556
6. Al-Jallad H, Palomo T, Roughley P, Glorieux FH, McKee MD, Moffatt P, Rauch F (2015) The effect of SERPINF1 in-frame mutations in osteogenesis imperfecta type VI. Bone 76:115–120
7. Al-Jallad H, Palomo T, Moffatt P, Roughley P, Glorieux FH, Rauch F (2014) Normal bone density and fat mass in

heterozygous SERPINF1 mutation carriers. J Clin Endocrinol Metab 99:E2446–E2450
8. Kalkwarf HJ, Zemel BS, Yolton K, Heubi JE (2013) Bone mineral content and density of the lumbar spine of infants and toddlers: influence of age, sex, race, growth, and human milk feeding. J Bone Miner Res 28:206–212
9. Zemel BS, Kalkwarf HJ, Gilsanz V, Lappe JM, Oberfield S, Shepherd JA, Frederick MM, Huang X, Lu M, Mahboubi S, Hangartner T, Winer KK (2011) Revised reference curves for bone mineral content and areal bone mineral density according to age and sex for black and non-black children: results of the bone mineral density in childhood study. J Clin Endocrinol Metab 96:3160–3169
10. Glorieux FH, Travers R, Taylor A, Bowen JR, Rauch F, Norman M, Parfitt AM (2000) Normative data for iliac bone histomorphometry in growing children. Bone 26:103–109
11. Rauch F, Lalic L, Glorieux FH, Moffatt P, Roughley P (2014) Targeted sequencing of a pediatric metabolic bone gene panel using a desktop semiconductor next-generation sequencer. Calcif Tissue Int 95:323–331
12. Schleit J, Bailey SS, Tran T, Chen D, Stowers S, Schwarze U, Byers PH (2015) Molecular outcome, prediction, and clinical consequences of splice variants in COL1A1, which encodes the proalpha1(I) chains of type I procollagen. Hum Mutat 36:728–739
13. Meyer C, Notari L, Becerra SP (2002) Mapping the type I collagen-binding site on pigment epithelium-derived factor. Implications for its antiangiogenic activity. J Biol Chem 277:45400–45407
14. Fratzl-Zelman N, Schmidt I, Roschger P, Roschger A, Glorieux FH, Klaushofer K, Wagermaier W, Rauch F, Fratzl P (2015) Unique micro- and nano-scale mineralization pattern of human osteogenesis imperfecta type VI bone. Bone 73:233–241
15. Roschger P, Fratzl-Zelman N, Misof BM, Glorieux FH, Klaushofer K, Rauch F (2008) Evidence that abnormal high bone mineralization in growing children with osteogenesis imperfecta is not associated with specific collagen mutations. Calcif Tissue Int 82:263–270
16. Hoyer-Kuhn H, Netzer C, Koerber F, Schoenau E, Semler O (2014) Two years' experience with denosumab for children with osteogenesis imperfecta type VI. Orphanet J Rare Dis 9:145
17. Brown JP, Reid IR, Wagman RB, Kendler D, Miller PD, Jensen JE, Bolognese MA, Daizadeh N, Valter I, Zerbini CA, Dempster DW (2014) Effects of up to 5 years of denosumab treatment on bone histology and histomorphometry: the FREEDOM study extension. J Bone Miner Res 29:2051–2056
18. Bone HG, Bolognese MA, Yuen CK, Kendler DL, Miller PD, Yang YC, Grazette L, San Martin J, Gallagher JC (2011) Effects of denosumab treatment and discontinuation on bone mineral density and bone turnover markers in postmenopausal women with low bone mass. J Clin Endocrinol Metab 96:972–980

Web Resources

Exome Aggregation Consortium (ExAC) Browser: http://exac.broadinstitute.org/
Human Splice Finder, version 3.0: http://www.umd.be/HSF3/
Online Mendelian Inheritance in Man (OMIM): http://www.omim.org
Osteogenesis Imperfecta Variant Database: http://www.le.ac.uk/ge/collagen/